

CHANNEL, TREND AND PERIODIC-WISE REPRESENTATION LEARNING FOR MULTIVARIATE LONG-TERM TIME SERIES FORECASTING

Zhangyao Song^{*}, Nanqing Jiang^{*}, Miaohong He, Xiaoyu Zhao, Tao Guo[✉]

School of Cyber Science and Engineering, Southeast University, Nanjing, China

ABSTRACT

Downsampling-based methods for time series forecasting have gained significant attention due to their effectiveness in capturing sequence trends. However, these approaches primarily focus on dependencies within subsequences, neglecting inter-subsequence and inter-channel interactions, which limits forecasting accuracy. To overcome these limitations, we propose CTPNET, a novel framework that explicitly learns representations from three complementary perspectives: i) inter-channel dependencies, captured by a temporal query-based multi-head attention mechanism; ii) intra-subsequence dependencies, modeled via a Transformer to characterize trend variations; and iii) inter-subsequence dependencies, extracted by reusing the encoder with residual connections to capture global periodic patterns. By jointly integrating these levels, the proposed method provides a holistic representation of temporal dynamics. Extensive experiments on multiple real-world datasets demonstrate the superiority and robustness of CTPNET, establishing new state-of-the-art performance in long-term time series forecasting.

Index Terms— Time series forecasting, downsampling, multi-scale dependencies, Transformer.

1. INTRODUCTION

Time series forecasting aims to predict future values based on historical time series data and has significant applications in fields such as energy management [1], weather forecasting [2], and traffic monitoring [3, 4]. Furthermore, multivariate long-term time series forecasting has garnered increasing attention due to its ability to provide richer future insights and leverage dependencies between multiple variables [5–7]. With advancements in deep learning, various methods have been proposed for multivariate long-term time series forecasting, including those based on Recurrent Neural Networks (RNNs) [8, 9], Convolutional Neural Networks (CNNs) [7, 10–12], Multi-layer Perceptrons (MLPs) [13, 14], and Transformers [4, 15, 16]. However, the complexity of real-world time series data often limits the effectiveness of these methods.

Accurate long-term time series forecasting fundamentally relies on capturing the inherent inter-channel dependencies and temporal dependencies within the data. Temporal dependencies can be further categorized into trends and periodic patterns. For inter-channel dependencies, recent studies [5, 6, 15] have utilized attention mechanisms due to their strong capability to extract multi-level representations. For temporal dependencies, a common strategy [17–19] is to down-sample (see Fig. 1b) the time series into subsequences based on periodicity, which has demonstrated strong predictive capabilities. At

this stage, each subsequence captures the trend variations of the time series, while relationships across subsequences reflect periodic dependencies. For instance, [17] employs a weight-shared MLP to extract intra-subsequence dependencies. Since time series often exhibit fixed periodic patterns (e.g., daily cycles), each downsampled subsequence tends to display consistent trends. However, this approach primarily focuses on dependencies within individual subsequences, neglecting inter-subsequence dependencies, which leads to the loss of valuable temporal information. Moreover, it overlooks the modeling of inter-channel dependencies [20]. These limitations raise a fundamental question: how can we design a forecasting framework that effectively learns comprehensive temporal representations across inter-channel, intra-subsequence, and inter-subsequence dependencies?

In this paper, we address these limitations by proposing CTPNET (Channel, Trend, and Period-wise representation learning Network), a novel framework that performs representation learning on three complementary levels of dependencies: i) I_1 inter-channel dependencies, which capture interactions across variables; ii) I_2 intra-subsequence dependencies, which model local temporal structures within each subsequence; and iii) I_3 inter-subsequence dependencies, which uncover global temporal dynamics across subsequences. Specifically, for inter-channel dependencies, we employ a temporal query-based [5] Multi-Head Attention (MHA) [21]. By using a learnable query matrix Q , the MHA mechanism effectively captures cross-channel dependencies. For intra-subsequence dependencies, we adopt a Transformer with linear complexity [22]. The residual connection [23] between the inter-channel dependencies and the original input, followed by linear encoding [13], is used as the Query, Key, and Value of the attention mechanism. This enables the Transformer to effectively capture complex trend variations (i.e., intra-subsequence dependencies) in the high-dimensional hidden space. Finally, for inter-subsequence dependencies, we use the same network as before. By inputting the transposed encoder output with a residual connection to I_2 , the network can model inter-subsequence dependencies.

Using these three perspectives together, CTPNET offers a holistic representation of time series data, overcoming the limitations of previous methods. Extensive experiments conducted on multiple benchmark datasets demonstrate the superiority of our approach. In summary, our contributions are threefold:

- Unlike previous methods that only exploit intra-subsequence dependencies within downsampled subsequences, we explicitly model inter-subsequence dependencies.
- We propose CTPNET, a unified framework that simultaneously learns inter-channel, intra-subsequence, and inter-subsequence dependencies for comprehensive representation.
- Through extensive experiments, we establish new state-of-the-art performance across multiple benchmarks, demonstrating the robustness and generality of our framework.

This work was supported in part by the NSFC Project 62301144, and in part by the Zhishan Young Scholar Fund No.2242025RCB0032. The first two authors are equally contributed. (Corresponding author: Tao Guo, taoguo@seu.edu.cn). [Code](#)

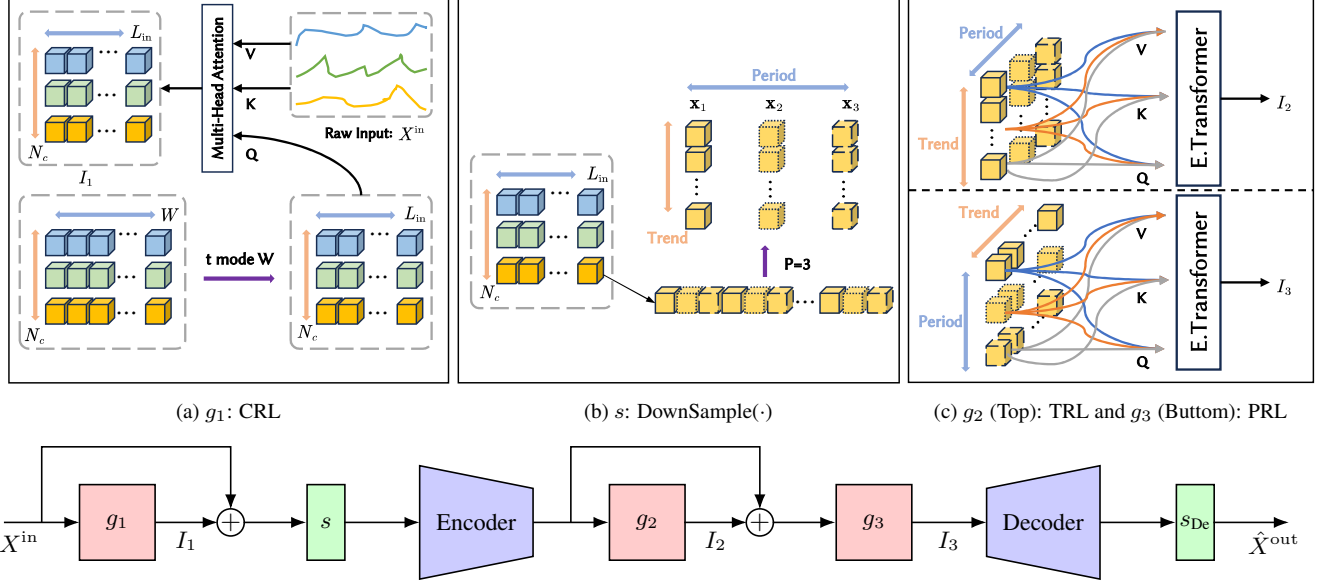


Fig. 1: Overview of CTPNET. Here g_1 , g_2 and g_3 represent the representation learning networks for inter-channel dependencies, intra-subsequence dependencies, and inter-subsequence dependencies, respectively. s denotes $\text{DownSample}(\cdot)$, and s_{De} denotes its inverse process.

2. PRELIMINARIES

2.1. Problem Statement

Given a historical series $X^{\text{in}} = [x_t^{(1:N_c)}, \dots, x_{t-L_{\text{in}}-1}^{(1:N_c)}] \in \mathbb{R}^{N_c \times L_{\text{in}}}$ of L_{in} time steps with N_c channels (e.g., the number of variables), the goal of time series forecasting (TSF) is to predict the series $\hat{X}^{\text{out}} = [\hat{x}_{t+L_{\text{out}}}^{(1:N_c)}, \dots, \hat{x}_{t+1}^{(1:N_c)}] \in \mathbb{R}^{N_c \times L_{\text{out}}}$ for the next L_{out} time steps based on X^{in} , while minimizing the difference between \hat{X}^{out} and the target X^{target} . This can be formulated as:

$$[\hat{x}_{t+L_{\text{out}}}^{(1:N_c)}, \dots, \hat{x}_{t+1}^{(1:N_c)}] = f([x_t^{(1:N_c)}, \dots, x_{t-L_{\text{in}}-1}^{(1:N_c)}]), \quad (1)$$

where f represents a trainable neural network.

2.2. Time Series Downsampling

Given a time series $X = [x_t^{(n)}, \dots, x_{t-L_{\text{in}}-1}^{(n)}]$ with periodicity P , the operation of downsampling [17] decomposes the sequence into P downsampled subsequences of length $N_{\text{pin}} = \lfloor \frac{L_{\text{in}}}{P} \rfloor$. As illustrated in Fig. 1b, this process can be expressed as:

$$[\mathbf{x}_1, \dots, \mathbf{x}_P] = \text{DownSample}(X), \quad (2)$$

where $\mathbf{x}_p = [x_{t+p-1+0 \times P}, \dots, x_{t+p-1+(N_{\text{pin}}-1) \times P}] \in \mathbb{R}^{N_{\text{pin}}}$ denotes the p -th subsequence. The inverse process of $\text{DownSample}(\cdot)$ is denoted as $\text{De-DownSample}(\cdot)$.

3. METHOD: CTPNET

3.1. Structure Overview

As illustrated in Fig. 1, the proposed CTPNET consists of seven key components: ① **Channel-wise Representation Learning (CRL)** captures inter-channel dependencies; ② $\text{DownSample}(\cdot)$ downsamples the residual connection of I_1 and the original input to generate multiple subsequences; ③ **Encoder** maps each subsequence of length

N_{pin} into a D -dimensional representation; ④ **Trend-wise Representation Learning (TRL)** captures intra-subsequence dependencies; ⑤ **Periodic-wise Representation Learning (PRL)** captures inter-subsequence dependencies; ⑥ **Decoder** converts the subsequence length from D back to N_{pout} , enabling the next operation to yield a prediction horizon of length L_{out} ; ⑦ $\text{De-Downsample}(\cdot)$ recombines the multiple subsequences into a single sequence.

3.2. Channel-wise Representation Learning (CRL)

We adopt the Temporal Query (TQ) [5] technique to model inter-channel dependencies I_1 . As shown in Fig. 1a, this method introduces periodically shifted learnable vectors as queries to mitigate the impact of noise and missing values on local correlations, while the raw input sequence serves as keys and values to preserve instance-level information. This allows the attention mechanism to integrate both global priors and local features. Specifically, given a period length W , we define the learnable parameters

$$\theta^{TQ} \in \mathbb{R}^{N_c \times W}, \quad (3)$$

and at time step t , a segment of length L_{in} is selected as the query:

$$Q = \theta_{t, L_{\text{in}}}^{TQ} \in \mathbb{R}^{N_c \times L_{\text{in}}}, \quad (4)$$

where the index is determined by $t \bmod W$, enabling periodic parameter reuse. The input sequence X_t is linearly projected to obtain keys and values:

$$K_1 = X_t W^{K_1}, \quad V_1 = X_t W^{V_1}, \quad (5)$$

and the attention is computed as:

$$\text{Head}_h = \text{Softmax}\left(\frac{Q_h K_h^T}{\sqrt{L_{\text{in}}}}\right) V_h. \quad (6)$$

The MHA mechanism concatenates the outputs:

$$I_1 = \text{MHA}(Q, K_1, V_1) = \text{Concat}(\text{head}_1, \dots, \text{head}_H) W^O, \quad (7)$$

where W^O is a learnable projection matrix.

Table 1
MULTIVARIATE TIME SERIES FORECASTING RESULTS

MODEL	METRIC	CTPNET (OURS)		TQNET [5] (2025)		TWINS* [24] (2025)		LEDDAM [20] (2024)		iTRANS* [15] (2024)		PATCHTST [16] (2023)		CROSS* [6] (2023)		FED* [1] (2022)	
		MSE	MAE	MSE	MAE	MSE	MAE	MSE	MAE	MSE	MAE	MSE	MAE	MSE	MAE	MSE	MAE
ETTH1	96	0.363	0.388	0.371	0.393	0.385	0.401	0.377	0.394	0.386	0.405	0.414	0.419	0.423	0.448	0.376	0.419
	192	0.414	0.416	0.428	0.426	0.439	0.431	0.424	<u>0.422</u>	0.441	0.436	0.460	0.445	0.471	0.474	<u>0.420</u>	0.448
	336	0.453	0.435	0.476	0.446	0.480	0.452	0.459	<u>0.442</u>	0.487	0.458	0.501	0.466	0.570	0.546	<u>0.459</u>	0.465
	720	0.451	0.451	0.487	0.470	0.480	0.474	<u>0.463</u>	<u>0.459</u>	0.503	0.491	0.500	0.488	0.653	0.621	<u>0.506</u>	0.507
ETTH2	96	0.287	0.336	0.295	0.343	0.292	0.345	<u>0.292</u>	<u>0.343</u>	0.297	0.349	0.302	0.348	0.745	0.584	0.358	0.397
	192	0.356	0.381	0.367	0.393	0.375	0.395	<u>0.367</u>	<u>0.389</u>	0.380	0.400	0.388	0.400	0.877	0.656	0.429	0.439
	336	0.412	0.422	0.417	0.427	0.417	0.429	0.412	<u>0.424</u>	0.428	0.432	0.426	0.433	1.043	0.731	0.496	0.487
	720	0.410	0.433	0.433	0.446	0.406	0.430	0.419	0.438	0.427	0.445	0.431	0.446	0.463	1.104	0.763	0.474
ETTM1	96	0.310	0.346	<u>0.311</u>	<u>0.353</u>	0.325	0.364	0.319	0.359	0.334	0.368	0.329	0.367	0.404	0.426	0.379	0.419
	192	0.359	0.376	0.356	<u>0.378</u>	0.372	0.390	0.369	0.383	0.377	0.391	0.367	0.385	0.450	0.451	0.426	0.441
	336	0.387	0.395	0.390	<u>0.401</u>	0.406	0.412	0.394	0.402	0.426	0.420	0.399	0.410	0.532	0.515	0.445	0.459
	720	0.449	0.434	<u>0.452</u>	0.440	0.467	0.448	0.460	0.442	0.491	0.459	0.454	<u>0.439</u>	0.666	0.589	0.543	0.490
ETTM2	96	0.174	0.251	0.173	<u>0.256</u>	0.173	0.256	0.176	0.257	0.180	0.264	0.175	0.259	0.287	0.366	0.203	0.287
	192	0.238	0.294	0.238	<u>0.298</u>	0.239	0.300	0.243	0.303	0.250	0.309	0.241	0.302	0.414	0.492	0.269	0.328
	336	0.299	0.333	0.301	0.340	0.298	0.339	0.303	0.341	0.311	0.348	0.305	0.343	0.597	0.542	0.325	0.366
	720	0.399	0.392	0.397	0.396	0.397	0.397	0.400	0.398	0.412	0.407	0.402	0.400	1.730	1.042	0.421	0.415
ECL	96	0.134	0.224	0.134	<u>0.229</u>	0.139	0.233	0.141	0.235	0.148	0.240	0.181	0.270	0.219	0.314	0.193	0.308
	192	0.151	0.240	0.154	<u>0.247</u>	0.158	0.252	0.159	0.252	0.162	0.253	0.188	0.274	0.231	0.322	0.201	0.315
	336	0.166	0.256	0.169	0.264	0.172	0.267	0.173	0.268	0.178	0.269	0.204	0.293	0.246	0.337	0.214	0.329
	720	0.200	0.286	0.201	0.294	0.200	0.293	0.201	0.295	0.225	0.317	0.246	0.324	0.280	0.363	0.246	0.355
SOLAR	96	0.168	0.223	0.173	0.233	0.193	0.224	0.197	0.241	0.203	0.237	0.234	0.286	0.310	0.331	0.242	0.342
	192	0.184	0.238	0.199	0.257	0.223	0.250	0.231	0.264	0.233	0.261	0.267	0.310	0.734	0.725	0.285	0.380
	336	0.200	0.254	0.211	0.263	0.246	0.268	0.241	0.268	0.248	0.273	0.290	0.315	0.750	0.735	0.282	0.376
	720	0.204	0.247	0.209	<u>0.270</u>	0.245	0.272	0.250	0.281	0.249	0.275	0.289	0.317	0.769	0.765	0.357	0.427
WEATHER TRAFFIC	96	0.398	0.251	0.413	0.261	0.382	0.260	0.426	0.276	0.395	0.268	0.462	0.290	0.522	0.290	0.587	0.366
	192	0.419	0.261	0.432	0.271	0.392	0.267	0.458	0.289	<u>0.417</u>	0.276	0.466	0.290	0.530	0.293	0.604	0.373
	336	0.436	0.270	0.450	0.277	0.410	<u>0.276</u>	0.486	0.297	<u>0.433</u>	0.283	0.482	0.300	0.558	0.305	0.621	0.383
	720	0.470	0.291	0.486	0.295	0.442	<u>0.292</u>	0.498	0.313	<u>0.467</u>	0.302	0.514	0.320	0.589	0.328	0.626	0.382
1 st COUNT	96	0.156	0.196	0.157	0.200	0.161	0.201	0.156	0.202	0.174	0.214	0.177	0.210	0.158	0.230	0.217	0.296
	192	0.204	0.241	0.206	<u>0.245</u>	0.211	0.248	0.207	0.250	0.221	0.254	0.225	0.250	<u>0.206</u>	0.277	0.276	0.336
	336	0.262	0.285	0.262	<u>0.287</u>	0.266	0.291	0.262	0.291	0.278	0.296	0.278	0.290	0.272	0.335	0.339	0.380
	720	0.343	0.340	0.344	0.342	0.347	0.343	0.343	0.343	0.358	0.349	0.354	0.340	0.398	0.418	0.403	0.428

The look-back length L_{in} is fixed at 96, and "*" denotes "former".

Remark 1. It is worth noting that the period W here differs from the one used in downsampling. For downsampling, a large period would result in overly sparse sequences and loss of temporal information; thus, the smallest inherent period (e.g., daily period of 24) is usually adopted. In contrast, in the TQ mechanism, the query Q is designed to capture long-range periodic variations, and therefore a longer period (e.g., weekly period of 168) is preferred. Both types of periods can be determined via the autocorrelation function (ACF) [25].

We perform a residual connection between I_1 and the original input X^{in} , formulated as:

$$X^{in'} \in \mathbb{R}^{N_c \times L_{in}} = X^{in} + I_1, \quad (8)$$

to enhance training stability. After that, downsampling (as introduced in Section 2.2) is applied:

$$X_{ds}^{in'} \in \mathbb{R}^{N_c \times P \times N_{pin}} = \text{DownSample}(X^{in'}), \quad (9)$$

and the resulting P subsequences are fed into the following networks.

3.3. Trend-wise Representation Learning (TRL)

The downsampled subsequences are processed by a linear encoder, which maps the temporal dimension after downsampling into a D -dimensional hidden space:

$$Z \in \mathbb{R}^{N_c \times P \times D} = \text{Encoder}(X_{ds}^{in'}). \quad (10)$$

Prior studies [13, 14, 17] have shown that this setup allows neural networks to extract richer features in the higher-dimensional hidden space while alleviating the sparsity issue caused by wide

intervals in downsampling. Afterward, the TRL network captures intra-subsequence temporal dependencies I_2 within the hidden space, as illustrated in Fig. 1c Top. Specifically, we adopt an efficient attention [22] to extract I_2 , defined as:

$$E_2 = \text{Attention}(Q_2, K_2, V_2) = \rho(Q_2) \left(\rho(K_2^T) \cdot V_2 \right), \quad (11)$$

where $\rho(\cdot)$ denotes $\frac{\cdot}{\sqrt{\dim(\cdot)}}$ and:

$$Q_2 = ZW^{Q_2}, \quad K_2 = ZW^{K_2}, \quad V_2 = ZW^{V_2}, \quad (12)$$

with $W^{Q_2}, W^{K_2}, W^{V_2}$ being learnable weight matrices. E_2 is input into an MHA, following an operation similar to that in Eq. (13), to obtain $E_2^{(mha)}$. Then, $E_2^{(mha)}$ is input into the Transformer network:

$$\begin{aligned} I_2' &= \text{LayerNorm}(Z + E_2^{(mha)}), \\ I_2'' &= \text{Linear}(\text{GELU}(\text{Linear}(I_2'))), \\ I_2 &= \text{LayerNorm}(I_2' + I_2''), \end{aligned} \quad (13)$$

where $\text{Linear}(\text{GELU}(\text{Linear}(\cdot)))$ represents a multi-layer feedforward network, and $\text{LayerNorm}(\cdot)$ denotes layer normalization.

3.4. Periodic-wise Representation Learning (PRL)

The network used to extract I_3 has the same structure as the network used to extract I_2 . When the feature dimensions input to the network differ, it is capable of capturing dependencies of different dimensions. To extract I_3 , a transpose is first performed to move the subsequence dimension to the last axis, as illustrated in Fig. 1c bottom. At the

Table 2
ABLATION RESULTS OF CTPNET

ABLATION	FULL	I_1	I_2	I_3	I_1, I_2	I_1, I_3	I_2, I_3
ETTh2	MSE	0.366	0.369	0.371	0.384	0.375	0.380
	MAE	0.393	<u>0.395</u>	0.396	0.402	0.399	0.400
ETTM2	MSE	0.278	<u>0.279</u>	0.280	0.281	0.285	0.287
	MAE	0.318	<u>0.320</u>	0.320	0.320	0.327	0.324
ECL	MSE	0.163	0.190	<u>0.170</u>	0.176	0.201	0.207
	MAE	0.252	0.270	<u>0.258</u>	0.265	0.278	0.284
SOLAR	MSE	0.189	0.221	<u>0.193</u>	0.197	0.265	0.264
	MAE	0.241	0.260	<u>0.243</u>	0.254	0.320	0.310
TRAFFIC	MSE	0.431	0.454	<u>0.462</u>	<u>0.448</u>	0.509	0.510
	MAE	0.268	<u>0.278</u>	0.282	0.292	0.306	0.321

The results are averaged over four prediction horizons.

same time, the operations in Equations (11) to (13) are carried out, which we denote concisely as:

$$I_3 = g_3 \left((Z + I_2)^\top \right)^\top. \quad (14)$$

At this point, the network can effectively extract I_3 . Subsequently, the linear decoder projects the learned representations onto the target prediction time domain:

$$\hat{X}_{ds}^{out} = \text{Decoder}(I_3). \quad (15)$$

It then combines them through inverse downsampling:

$$\hat{X}^{out} = \text{De-DownSample}(\hat{X}_{ds}^{out}), \quad (16)$$

to form a predicted tensor of length L_{out} , where $\hat{X}^{out} \in \mathbb{R}^{N_c \times L_{out}}$ denotes the predicted results.

4. EXPERIMENT

The performance of the proposed CTPNET is evaluated on eight widely used benchmark datasets, including ETT (ETTh1, ETTh2, ETTm1, ETTm2), Weather, Electricity (ECL), Traffic, and Solar. The data preprocessing procedure follows prior works [5], including the instance normalization strategy. All experiments were implemented using the PyTorch framework and executed on an NVIDIA RTX 4090 GPU equipped with 24 GB of memory. The training objective used an L1 loss function optimized with the Adam optimizer [26].

4.1. Long-term Forecasting

Setup. We evaluated the performance of CTPNET against seven mainstream methods, including TQNet [5], Twinsformer [27], Leddam [20], iTransformer [15], PatchTST [16], Crossformer [6], and FEDformer [1]. For long-term forecasting, following prior works [4, 5, 15, 28], we set the prediction horizons to $L_{out} \in \{96, 192, 336, 720\}$, while fixing the look-back window length to $L_{in} = 96$. Mean Squared Error (MSE) and Mean Absolute Error (MAE) were employed as evaluation metrics. The best results are highlighted in **bold**, while the second-best results are underlined.

Result Analysis. As shown in Table 1, CTPNET consistently achieves state-of-the-art performance, obtaining the lowest average MSE and MAE across all datasets and prediction horizons. Specifically, compared with TQNet [5] and Crossformer [6], CTPNET reduces MSE/MAE by 2.22%/2.45% and 19.37%/19.29%, respectively, on average. On datasets with pronounced periodic variations (ETTh1, ETTh2, and Solar), CTPNET outperforms the runner-up TQNet, reducing MSE/MAE by 4.76%/2.53%, 3.17%/2.24%, and 4.55%/5.86%, respectively. Overall, CTPNET ranks within the top two in 58 out of 64 evaluation metrics, including 54 first-place results.

Table 3
PERFORMANCE OF DIFFERENT INTERVAL ON ETTh1

INTERVAL HORIZON	MSE	MAE	MSE	MAE	MSE	MAE	MSE	MAE	MSE	MAE
	2	4	8	16	24					
96	0.373	0.392	0.373	0.392	0.370	0.389	0.386	0.398	0.363	0.388
192	0.425	0.420	<u>0.422</u>	<u>0.420</u>	0.431	0.425	0.436	0.428	0.414	0.416
336	0.464	0.438	<u>0.460</u>	<u>0.437</u>	0.494	0.462	0.482	0.456	0.453	0.435
720	<u>0.465</u>	<u>0.458</u>	<u>0.465</u>	<u>0.461</u>	0.553	0.509	0.480	0.473	0.451	0.451

Complexity Analysis. CTPNET balances computational efficiency and prediction accuracy by leveraging downsampling to reduce sequence length and adopting Efficient Attention to lower complexity from $O(n^2)$ to $O(n)$. These optimizations make CTPNET a robust choice for long-term time series forecasting.

4.2. Ablation Studies

4.2.1. Ablation on I_1 , I_2 , and I_3

As shown in Table 2, removing I_1 , I_2 , or I_3 individually results in a significant accuracy loss. For instance, on the ETTh2 and ETTm2 datasets, the highest accuracy loss occurs when I_3 is removed, highlighting the importance of inter-subsequence dependencies in datasets with clear periodic variations. Conversely, removing I_1 has the least impact on ETT datasets, which have only seven channels and relatively weak inter-channel dependencies. However, in datasets with a large number of channels, such as ECL ($N_c = 321$), Solar ($N_c = 137$), and Traffic ($N_c = 862$), removing I_1 leads to a more significant accuracy loss, verifying the effectiveness of inter-channel dependencies.

Furthermore, removing any two of I_1 , I_2 , and I_3 simultaneously leads to a greater accuracy drop, with the largest reduction observed when I_2 and I_3 are removed together. This highlights the necessity of modeling both intra-subsequence and inter-subsequence dependencies, as the ablated models consistently underperform compared to the full model.

4.2.2. Impact of Downsampling Interval

This section examines the impact of setting incorrect downsampling intervals on model performance. We conducted ablation experiments on the ETTh1 dataset using different fixed periods (2, 4, 8, 16, 24). Notably, the minimum period calculated via the autocorrelation function (ACF) is 24 (daily period). As shown in Table 3, when the downsampling interval is set to 24, the model achieves the best performance, demonstrating that aligning the downsampling interval with the data’s inherent periodicity enhances the capture of periodic patterns. Additionally, smaller downsampling intervals (e.g., 2 or 4) also yield competitive results, likely due to their ability to capture finer-grained trends in the time series.

5. CONCLUSION

In this paper, we tackled the challenge of capturing complex dependencies in time series forecasting. Unlike existing approaches that primarily focus on temporal dependencies within downsampled subsequences, we emphasized the importance of inter-subsequence dependencies. To address this, we proposed CTPNET, a novel framework that simultaneously models inter-channel, intra-subsequence, and inter-subsequence dependencies, enabling a more comprehensive representation of time series data. Extensive experiments conducted on multiple real-world datasets demonstrated the effectiveness and robustness of our method, establishing new state-of-the-art performance in long-term time series forecasting.

References

- [1] T. Zhou, Z. Ma, Q. Wen, et al., “FEDFormer: Frequency enhanced decomposed transformer for long-term series forecasting,” in *International Conference on Machine Learning*, 2022.
- [2] R. Ilbert, A. Odonnat, V. Feofanov, et al., “Samformer: Unlocking the potential of transformers in time series forecasting with sharpness-aware minimization and channel-wise attention,” in *Proceedings of the 41st International Conference on Machine Learning*, vol. 235, PMLR, 2024. [Online]. Available: <https://proceedings.mlr.press/v235/ilbert24a.html>
- [3] G. Woo, C. Liu, D. Sahoo, et al., “ETSformer: Exponential smoothing transformers for time-series forecasting,” *arXiv preprint arXiv:2202.01381*, 2022.
- [4] H. Zhou, S. Zhang, J. Peng, et al., “Informer: Beyond efficient transformer for long sequence time-series forecasting,” in *Proceedings of the AAAI Conference on Artificial Intelligence*, 2021.
- [5] S. Lin, H. Chen, H. Wu, et al., “Temporal query network for efficient multivariate time series forecasting,” in *Forty-second International Conference on Machine Learning*, 2025.
- [6] Y. Zhang and J. Yan, “Crossformer: Transformer utilizing cross-dimension dependency for multivariate time series forecasting,” in *International Conference on Learning Representations*, 2023.
- [7] E. Zhang, W. Yuan, and X. Liu, “ChannelMixer: A Hybrid CNN-Transformer Framework for Enhanced Multivariate Long-Term Time Series Forecasting,” in *IEEE International Conference on Acoustics, Speech and Signal Processing (ICASSP'2025)*, Hyderabad, India, April 6-11, 2025: IEEE, 2025, pp. 1–5. DOI: 10.1109/ICASSP49660.2025.10887797
- [8] S. Lin, W. Lin, W. Wu, et al., “SegRNN: Segment Recurrent Neural Network for Long-Term Time Series Forecasting,” *IEEE Internet of Things Journal*, pp. 1–1, 2025. DOI: 10.1109/JIOT.2025.3647705
- [9] X. Zhang, C. Zhong, J. Zhang, et al., “Robust recurrent neural networks for time series forecasting,” *Neurocomputing*, 2023.
- [10] L. donghao and wang xue, “ModernTCN: A modern pure convolution structure for general time series analysis,” in *The Twelfth International Conference on Learning Representations*, 2024. [Online]. Available: <https://openreview.net/forum?id=vpJMJerXHU>
- [11] S. Bai, J. Z. Kolter, and V. Koltun, “An empirical evaluation of generic convolutional and recurrent networks for sequence modeling,” *arXiv preprint arXiv:1803.01271*, 2018.
- [12] M. Liu, A. Zeng, M. Chen, et al., “SCINet: Time series modeling and forecasting with sample convolution and interaction,” *Advances in Neural Information Processing Systems*, 2022.
- [13] A. Zeng, M. Chen, L. Zhang, et al., “Are transformers effective for time series forecasting?” In *Proceedings of the AAAI Conference on Artificial Intelligence*, 2023.
- [14] S. Lin, W. Lin, X. Hu, et al., “Cyclenet: Enhancing time series forecasting through modeling periodic patterns,” *Advances in Neural Information Processing Systems*, vol. 37, pp. 106 315–106 345, 2024.
- [15] Y. Liu, T. Hu, H. Zhang, et al., “iTransformer: Inverted transformers are effective for time series forecasting,” in *The Twelfth International Conference on Learning Representations*, 2024.
- [16] Y. Nie, N. H. Nguyen, P. Sinthong, et al., “A time series is worth 64 words: Long-term forecasting with transformers,” in *International Conference on Learning Representations*, 2023.
- [17] S. Lin, W. Lin, W. Wu, et al., “SparseTSF: Modeling long-term time series forecasting with 1k parameters,” in *Forty-first International Conference on Machine Learning*, 2024.
- [18] H. Wu, T. Hu, Y. Liu, et al., “TimesNet: Temporal 2d-variation modeling for general time series analysis,” in *International Conference on Learning Representations*, 2023.
- [19] S. Wang, J. LI, X. Shi, et al., “Timemixer++: A general time series pattern machine for universal predictive analysis,” in *The Thirteenth International Conference on Learning Representations*, 2025. [Online]. Available: <https://openreview.net/forum?id=1CLzLXSFNn>
- [20] G. Yu, J. Zou, X. Hu, et al., “Revitalizing multivariate time series forecasting: Learnable decomposition with Inter-Series dependencies and intra-series variations modeling,” in *Forty-first International Conference on Machine Learning*, 2024.
- [21] A. Vaswani, N. Shazeer, N. Parmar, et al., “Attention Is All You Need,” in *Advances in Neural Information Processing Systems*, 2017.
- [22] Z. Shen, M. Zhang, H. Zhao, et al., “Efficient attention: Attention with linear complexities,” *CoRR*, vol. abs/1812.01243, 2018. [Online]. Available: <http://arxiv.org/abs/1812.01243>
- [23] K. He, X. Zhang, S. Ren, et al., “Deep residual learning for image recognition,” in *Proceedings of the IEEE conference on computer vision and pattern recognition*, 2016, pp. 770–778.
- [24] A. Stitsyuk and J. Choi, “Xpatch: Dual-stream time series forecasting with exponential seasonal-trend decomposition,” in *Proceedings of the AAAI Conference on Artificial Intelligence*, vol. 39, 2025, pp. 20 601–20 609.
- [25] H. Madsen, *Time series analysis*. CRC Press, 2007.
- [26] D. P. Kingma and J. Ba, “Adam: A method for stochastic optimization,” *CoRR*, vol. abs/1412.6980, 2014. [Online]. Available: <https://api.semanticscholar.org/CorpusID:6628106>
- [27] Y. Zhou, Y. Ye, P. Zhang, et al., *Twinsformer: Revisiting inherent dependencies via two interactive components for time series forecasting*, 2025. [Online]. Available: <https://openreview.net/forum?id=BSsyY29bcl>
- [28] H. Wu, J. Xu, J. Wang, et al., “Autoformer: Decomposition transformers with auto-correlation for long-term series forecasting,” *Advances in Neural Information Processing Systems*, 2021.